Original Article
J Liver Cancer 2025;25(1):123-133
pISSN 2288-8128 • eISSN 2383-5001
https://doi.org/10.17998/jlc.2025.03.08

Identification of new biomarkers of hepatic cancer stem cells through proteomic profiling

Sung Hoon Choi[1,2], Ha Young Lee[3], Sung Ho Yun[3], Sung Jae Jang[1,4], Seung Up Kim[5,6], Jun Yong Park[5,6], Sang Hoon Ahn[5,6], Do Young Kim[5,6]

[1]Institute of Health & Environment, Seoul National University, Seoul, Korea
[2]KoBioLabs Inc., Seoul, Korea
[3]Digital Omics Research Center, Ochang Institute of Biological and Environmental Science, Korea Basic Science Institute, Cheongju, Korea
[4]Department of Environmental Health Sciences, Seoul National University Graduate School of Public Health, Seoul, Korea
[5]Department of Internal Medicine, Yonsei University College of Medicine, Seoul, Korea
[6]Yonsei Liver Cancer Center, Yonsei Cancer Hospital, Seoul, Korea

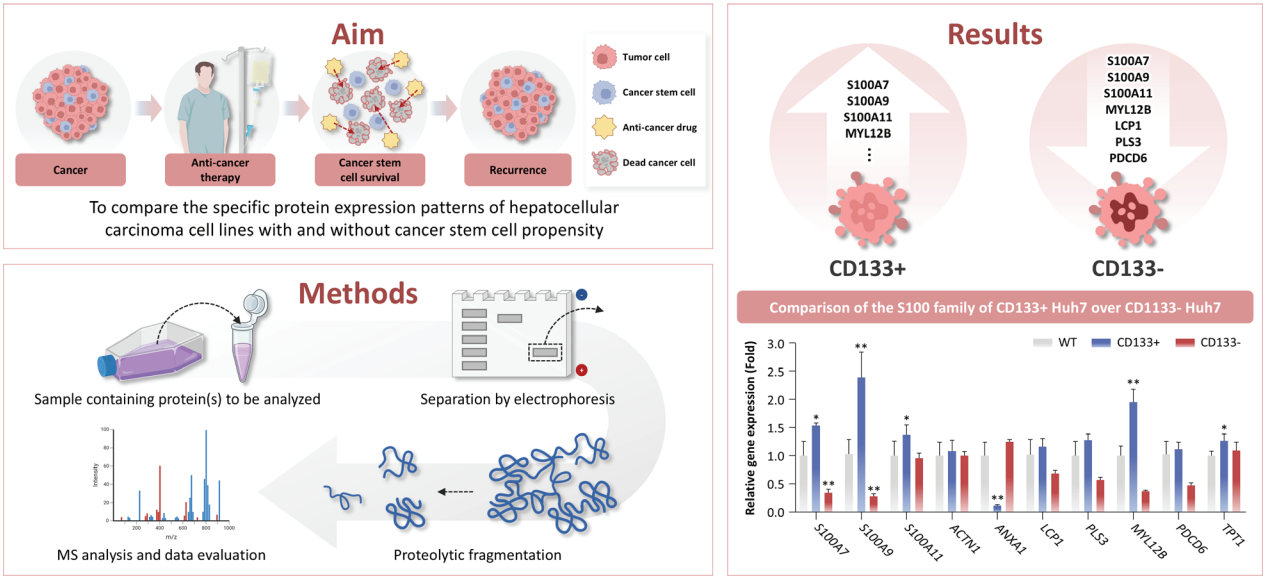

Conclusion

The S100 family proteins are new biomarkers of hepatic cancer stem cells, and are key factors in identifying novel therapeutic strategies for cancer stem cell metastasis and tumor progression.

Received Dec. 23, 2024 • **Revised** Feb. 28, 2025 • **Accepted** Mar. 8, 2025

Corresponding author: Do Young Kim
Department of Internal Medicine, Yonsei University College of Medicine, 50-1 Yonsei-ro, Seodaemun-gu, Seoul 03722, Korea
E-mail: dyk1025@yuhs.ac

Identification of new biomarkers of hepatic cancer stem cells through proteomic profiling

Sung Hoon Choi[1,2], Ha Young Lee[3], Sung Ho Yun[3], Sung Jae Jang[1,4], Seung Up Kim[5,6], Jun Yong Park[5,6], Sang Hoon Ahn[5,6], Do Young Kim[5,6]

Backgrounds/Aims: In hepatocellular carcinoma (HCC), which exhibits high mortality and recurrence rates globally, the traits of cancer stem cells (CSCs) that significantly influence recurrence and metastasis are not well understood. CSCs are self-renewing cell types identified in most liquid and solid cancers, contributing to tumor initiation, growth, resistance, recurrence, and metastasis following chemo-radiotherapy or trans-arterial chemoembolization therapy.

Methods: CSCs are classified based on the expression of cell surface markers such as CD133, which varies depending on the tumor type. Proteomic analysis of liver cancer cell lines with cancer stem cell potential and HCC cancer cell lines lacking stem cell propensity was conducted to compare and analyze specific expression patterns.

Results: Proteomic profiling and enrichment analysis revealed higher expression of the calcium-binding protein S100 family in CD133+ Huh7 cells than in CD133- or wild-type cells. Furthermore, elevated expression of S100 family members was confirmed in an actual CD133+ liver cancer cell line via protein-protein network analysis and quantitative polymerase chain reaction (qPCR).

Conclusion: The S100 family members are not only new markers of cancer stem cells but will also assist in identifying new treatment strategies for CSC metastasis and tumor advancement. **(J Liver Cancer 2025;25:123-133)**

Keywords: Carcinoma, hepatocellular; Neoplastic stem cells; Proteomic analysis; CD133-PROM1; S100 proteins

INTRODUCTION

Hepatocellular carcinoma (HCC) ranks as the sixth most prevalent cancer globally and is associated with poor prognosis owing to its malignant nature.[1] The progression of HCC is characterized by a gradual accumulation of genetic and epigenetic alterations, leading to common features, such as enhanced cell proliferation and evasion of apoptosis.[2] Although recent advancements in early detection and treatment have improved survival rates,[3] the challenges of recurrence and progression to malignancy continue to complicate the development of effective treatment strategies.[3]

The current perspective is that each primary tumor lesion is composed of cells that may differ genetically and epigenetically, resulting in phenotypic heterogeneity unique to each tumor type.[4] Some of these tumor cells, known as cancer stem cells (CSCs), are thought to be responsible for generating heterogeneous tumor lesions and contributing to treatment resistance, tumor relapse, and metastasis.[5]

CSCs contribute to tumor growth, maintenance, and recurrence after therapy through multiple mechanisms and networks.[6,7] An important feature of these cells is their ability to limit DNA damage caused by radiation or chemotherapy by reducing reactive oxygen species and increasing DNA checkpoint kinase activity.[8] By preventing DNA damage, the CSC population survives the injury and can continue to propagate within the tumor.[7] Additionally, CSCs play an important role in regulating tumor microenvironment to support cancer survival and metastasis through the modulation of various signaling pathways.[1,9]

Hepatic CSCs have emerged as key contributors to malignant tumors that recur after surgery or other treatments, such as transcatheter arterial chemoembolization or radiotherapy.[1,10,11] Analysis of CSC characteristics revealed that genetic alterations influenced by various external stimuli drive the malignant transformation of CSCs and play an important role in HCC treatment.[12] Therefore, in this study, we compared an HCC cell line with CSC propensity and an HCC cell line without stem cell propensity to identify specific characteristics and analyzed proteomic differences using proteomic methods to determine the propensities of liver CSCs.

MATERIALS AND METHODS

Cell culture

Huh-7 (KCLB60104; Korean Cell Line Bank, Seoul, Korea),

was cultured at 37°C with 5% CO_2 in Dulbecco's modified eagle medium (Gibco; Thermo Fisher Scientific, Waltham, MA, USA) supplemented with 10% fetal bovine serum (FBS) (Gibco; Thermo Fisher Scientific), 4.5 g/L glucose, L-glutamine, and 1% penicillin/streptomycin.

CD133+ and CD133- Huh7 cell isolation

Cells were harvested from Huh7 cell lines, and suspended in phosphate-buffered saline (PBS) supplemented with 2% FBS at a concentration of 1×10^7 cells/mL. The cells were then incubated with an anti-CD133 (W6B3C1; BioLegend, San Diego, CA, USA) antibody conjugated to fluorescein isothiocyanate (FITC) at the dilution recommended by the manufacturer for 30 min on ice in the dark. Following incubation, the cells were washed twice with PBS and 2% FBS to remove excess antibodies, and centrifuged at 300× g for 5 minutes. The resulting pellets were carefully resuspended in a small volume of PBS containing 2% FBS. The MACS system (Miltenyi Biotec, Bergisch Gladbach, Germany) was used according to the manufacturer's protocol as described.[13] A fluorescence-activated cell sorter (FACS) equipped with appropriate lasers and detectors was utilized for the selected fluorophores. The FACS was set to identify and sort CD133+ (positive) and CD133- (negative) populations based on fluorescence intensity. CD133+ cells were collected in one tube and CD133- cells in another. To confirm the purity of isolated populations, additional staining of sorted cells with anti-CD133 antibody was performed following FACS analysis. The percentage of CD133+ and CD133- cells in both sorted populations was assessed, with an expected purity greater than 90%. FACS analysis software (e.g., FlowJo) was used to determine the percentage and absolute count of CD133+ and CD133- cells in the populations (data not shown).

mRNA isolation and real-time quantitative polymerase chain reaction (RT-qPCR)

For RT-qPCR studies, cells were seeded in 6-well plates, allowed to adhere until reaching 85-90% confluence, and then incubated overnight in serum-containing conditions. The mRNA levels of human TERT, HKR3, and cell cycle factors were determined using SYBR green-based semi-quantitative PCR. RNA was extracted using a QIAGEN RNeasy Mini Kit (QIAGEN, Hilden, Germany) according to the manufacturer's instructions and reverse transcribed (RT) using a Clontech RT Kit (Clontech, Mountain View, CA, USA). Following reverse transcription, RT-qPCR analysis was performed using Applied Biosystems (Thermo Fisher Scientific) SYBR Green Master Mix and specific PCR primers (Supplementary Table 1). Amplification efficiencies were calculated for all primers using serial dilutions of the pooled cDNA samples. Data were analyzed using the comparative ΔΔCt method and normalized to beta-actin, the housekeeping gene. Results are presented as mean± standard error of the mean (SEM) (error bars) from at least three independent experiments and represented as fold-change relative to controls. Melting curves were generated to ensure the presence of a single gene-specific peak. No-template controls were included for each run, and each set of primers was used as a control for non-specific amplification.

PROTEOMIC ANALYSIS

Library preparation and sequencing

Total RNA was extracted using TRIzol® RNA Isolation Reagents (Life Technologies, Carlsbad, CA, USA). The quantity and quality of total RNA were evaluated using an Agilent 2100 Bioanalyzer RNA Kit (Agilent, Santa Clara, CA, USA). The isolated total RNA was processed to prepare an mRNA-sequencing library using the Illumina TruSeq Stranded mRNA Sample Preparation Kit (Illumina, San Diego, CA, USA) according to the manufacturer's protocol. Library quality and fragment size were assessed using an Agilent 2100 Bioanalyzer DNA Kit (Agilent). All libraries were quantified by qPCR using the CFX96 Real-Time System (Bio-Rad, Hercules, CA, USA) and sequenced on a NextSeq500 sequencer (Illumina) with a paired-end 75 bp read and a single 8 bp index read run.

Preprocessing and genome mapping

Potential sequencing adapters and law-quality bases in the raw reads were trimmed using Skewer software. The options -x AGATCGGAAGAGCACACGTCTGAACTCCAGTCA and -y AGATCGGAAGAGCGTCGTGTAGGGAAAGAGTGT were applied for removing common TruSeq adapter sequences (Illumina). Additionally, the parameters -q 0 -l 25 -k 3 -r 0.1 -d 0.1 were used to trim low-quality bases from the 5′ and 3′ ends of the raw reads. After trimming, the cleaned high-quality reads were mapped to the reference genome using STAR software. Because the sequencing libraries were prepared in a strand-specific manner using strand-specific library preparation kit (Illumina), the strand-specific library option, library-type=fr-

firststrand, was applied during the mapping process.

Quantifying gene expression and differentially expressed gene analysis

To quantify the mapped reads on the reference genome for gene expression analysis, Cufflinks with the strand-specific library option (library-type=fr-firststrand), and other default settings were used. The *hg19* gene annotation from the UCSC genome browser (https://genome.ucsc.edu) in GTF format was used as the gene model, and expression values were calculated in fragments per kilobase of transcript per million fragments mapped units. The differentially expressed genes between the two selected biological conditions were analyzed using Cuffdiff software in the Cufflinks package[5] with the strand-specific library option, (library-type=fr-firststrand) and other default settings. To compare the expression profiles among samples, the normalized expression values of a selected subset of a few hundred differentially expressed genes were clustered using unsupervised hierarchical clustering in in-house R scripts. Additionally, scatter plots for gene expression values and volcano plots for expression-fold changes and *P*-values were generated using in-house R scripts.

Functional category analysis

To gain insight into the biological functions associated with the differential gene expression between the compared biological conditions, a gene set overlapping test was performed between the analyzed differentially expressed genes and functionally categorized genes, including biological processes of gene ontology, KEGG pathways, and other functional gene sets using g:Profiler.

In-gel trypsin digestion

For the proteomic analysis, each group of samples was cultivated in triplicate under the conditions described above. The samples were dissolved using RIPA buffer. The protein concentration was determined by bicinchoninic acid (BCA) assay, and the samples were stored at -70°C for further study. A total of 15 μg of protein samples was separated using 12% sodium dodecyl sulfate-polyacrylamide gel electrophoresis (SDS-PAGE). The gels were fractionated into seven sections based on their molecular weights. In-gel digestion was performed as previously described.[14] The resulting tryptic peptides were dissolved in 0.5% trifluoroacetic acid for liquid chromatography with tandem mass spectrometry (LC-MS/MS) analysis.

Protein identification with LC-MS/MS analysis

Peptides were separated using an Ultimate 3000 UPLC system (Dionex, Sunnyvale, CA, USA) connected to a Q-Exactive Plus mass spectrometer (Thermo Fisher Scientific) equipped with a nanoelectrospray ion source (Dionex). Peptides were first concentrated on a trapping column (75 μm inner diameter) packed with 5 μm C18 particles (Acclaim PepMap; Thermo Fisher Scientific) and then separated using a 15 cm analytical column packed with RSLC C18 reversed-phase column (Thermo Fisher Scientific) at a flow rate of 300 nL/min. The peptides were eluted using a 0-95% acetonitrile gradient in 0.1% formic acid over 120 minutes. All MS and MS/MS spectra were acquired in the data-dependent top-10 mode, with automatic switching between full-scan MS and MS/MS acquisition. Survey full-scan MS spectra (m/z 150-2,000) were acquired using the Orbitrap at a resolution of 70,000 (m/z 200) after ion accumulation to a 1×10^6 target value based on predictive automatic gain control (AGC) from the previous full scan. The MS/MS analysis was performed three times for each sample. The raw MS/MS spectral files were converted to mgf files using the Proteome Discoverer Daemon ver.1.4 (Thermo Fisher Scientific). The converted mgf files were used for protein identification using MASCOT ver.2.4.1 (Matrix Science, Boston, MA, USA; www.matrixscience.com). Protein quantification was performed by calculating the exponentially modified protein abundance index (emPAI)[15] and the mol %, a percentile normalized value, based on the emPAI values. The search parameters applied in the database searches were as follows: enzyme specificity-trypsin/P, maximum missed cleavage-1, carboxymethyl as a static modification, oxidation and N-terminal acetylation as dynamic modifications, precursor mass tolerance of 10 ppm, and MS/MS mass tolerance of 0.8 Da. The MS/MS data were filtered according to a false discovery rate (FDR) of <1% to calculate the ratio of false positive matches in the decoy database based on the number of matches in the database. The UniProt human database (2018.05, www.uniprot.org), which has a total 93,614 sequences and 37,039,836 residues, was combined with cRAP database (2009.05.01, ftp://ftp.thegpm.org/fasta/cRAP/crap.fasta) which includes 116 sequences and 38,459 residues, and the contaminants database (2016.01.30, http://www.matrixscience.com/downloads/contaminants.zip), which consists of 247 sequences and 128,130 residues. These databases of common contaminants were used for protein identification. Relative quantitation and significance were provided for all the identified variables. Raw data are available via ProteomeXchange under the identifier PXD#331223 (https://www.ebi.

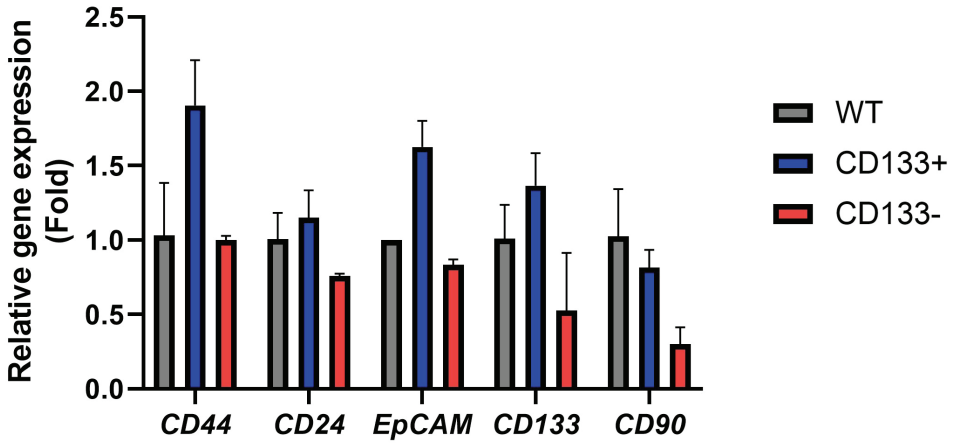

Figure 1. Identification of CD133+ and CD133- Huh7 cell lines. The CD133+ cell line was isolated from the HCC cell line Huh7, and a CD133- cell line lacking cancer stem cell propensity was also isolated. To confirm whether the isolated CD133+ Huh7 cell line had cancer stem cell line propensity, the expression of representative cancer stem cell markers CD44, CD24, EpCAM, and CD90 was assessed. WT, wild type; EpCAM, epithelial cell adhesion molecule.

ac.uk/pride/archive/).

Bioinformatic analysis

Functional analysis of the dataset was performed using protein network analysis (https://string-db.org/). The functional analysis identified the most significant biological functions and/or diseases associated with the dataset. The analysis was performed against the string test to calculate a *P*-value, determining the probability that each assigned biological function and/or disease was due to chance alone. The focus genes from the two shortlists were overlaid onto a global molecular network developed using the information contained in the STRING database. This generated network based on the connectivity of individual proteins. Simultaneously, protein clusters and assignments of differentially expressed genes were generated. To gain insight into the biological functional role of the differential gene expression between the compared biological conditions, a gene set overlapping test was performed. This test compared the differentially expressed genes with functionally categorized gene sets, including biological processes of Gene Ontology, KEGG pathways, and other functional gene sets using g:Profiler.

Statistical analysis

Results are expressed as means±SEM or frequency (%). An independent *t*-test was performed to compare the differences in means between the control and experimental groups. All statistical analyses were performed using SPSS version 12.0 (IMB, Armonk, NY, USA). Statistical significance was set at $P<0.05$.

RESULTS

Identification of CSC propensity in Huh7 cell lines

To analyze the propensity of CSCs specific to liver cancer, cell lines with CSC characteristics were isolated from HCC cell lines and confirmed to exhibit CSC properties. Based on CD133, a representative CSC marker, a CD133+ cell line was isolated from the HCC cell line Huh7, and a CD133- cell line lacking CSC characteristics was also isolated. To confirm whether the isolated CD133+ Huh7 cell line exhibited CSC propensity, the expression of the representative CSC markers CD44, CD24, epithelial cell adhesion molecule (EpCAM), and CD90 was analyzed (Fig. 1). Compared to wild-type Huh7 cells before isolation, EpCAM, CD44, and CD133 showed significantly higher expression patterns in the CD133+ Huh7 cell line, and although not significant, CD24 also showed high expression patterns. In contrast, CD90, which is recognized as a novel CSC marker in HCC, showed high expression overall but lower expression, although not significant, compared to the wild-type Huh7 cells. However, this was still higher than the CD133- cell line.

Proteomic profiling of CD133+ and CD133- Huh7

The proteomic profiling analysis of CD133+ Huh7, which expresses four out of five CSC markers, was compared with that of wild-type and CD133- cells. CD133+ HCC cell lines exhibited distinct expression patterns compared to wild-type or CD133- cells, while wild-type and CD133- cells showed similar expression patterns (Fig. 2A). In CD133+ cells, the expression of genes

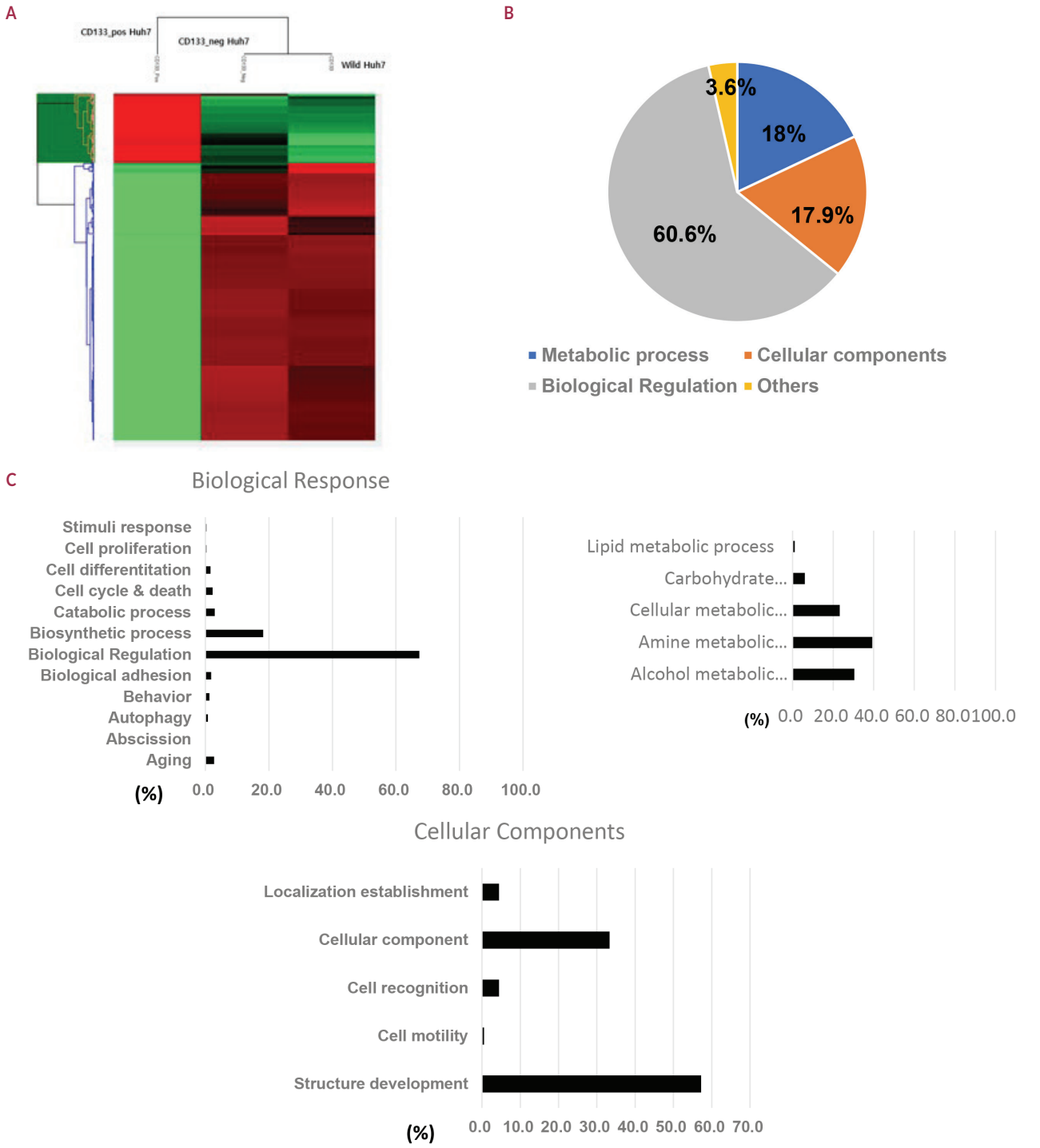

Figure 2. Proteomic profiling of CD133+ and CD133- Huh7 cell lines. The proteomic profiling analysis of CD133+ Huh7 was compared with wild-type and CD133- type. (A) CD133+ HCC cell lines showed distinct expression patterns compared to wild-type or CD133- type, while wild-type and CD133- cells showed similar expression patterns. (B) Proteomic profiling revealed various genetic changes, identifying four types of expression changes. The most significant expression difference was observed in biological regulation (approximately 61%). (C) Among the three categories (biological response, metabolic process, and cellular components) with major expression changes, we identified significant changes in biological regulation (approximately 64%), amine metabolic processes (approximately 40%), and structural development (approximately 58%). This profiling was conducted in duplicate analyses with high statistical significance. HCC, hepatocellular carcinoma.

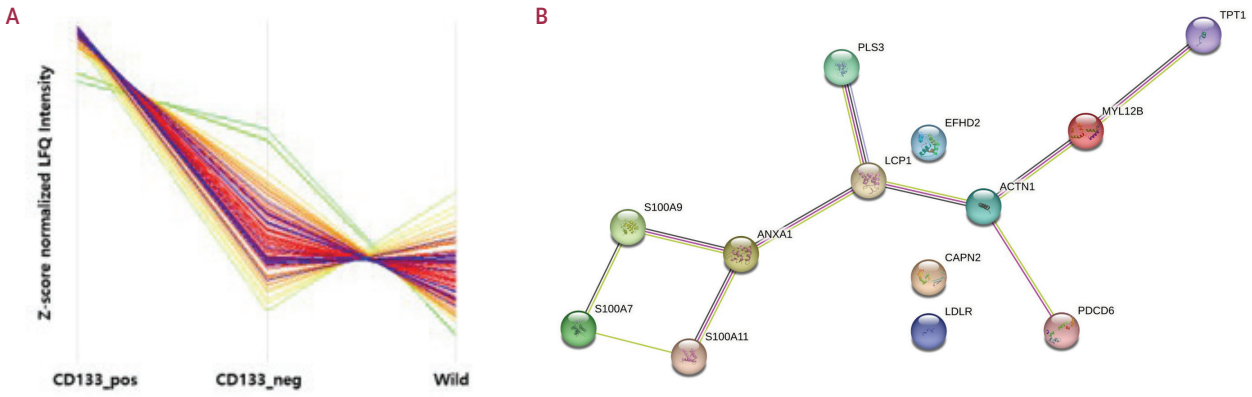

Figure 3. Enrichment network of CD133+ Huh7 and CD133- Huh7. (A) Labelling-free quantification (LFQ) of proteins compared mass spectral peak intensities between CD133+ and CD133- and confirmed that CD133- and wild-type had similar intensities, while CD133+ type had higher peak intensities that were different from that of CD133- and wild-type. (B) Analysis of the CD133+-specific protein network confirmed the network composition of various biological regulation-related proteins such as S100P.

Table 1. Enrichment protein network highly correlated with CD133+ HCC

Enrichment network protein	Gene
Calpain-2 catalytic subunit	*CAPN2*
Protein S100-A9	*S100A9*
EF-hand domain-containing protein D2	*EFHD2*
Plastin-2	*LCP1*
Protein S100-A11	*S100A11*
N-terminally processed	
Annexin A1 (Annexin)	*ANXA1*
Alpha-actinin-1	*ACTN1*
Low-density lipoprotein receptor	*LDLR*
Translationally-controlled tumor protein	*TPT1*
Protein S100-A7	*S100A7*
Programmed cell death protein 6	*PDCD6*
Myosin regulatory light chain 12B	*MYL12B*
Plastin-3	*PLS3*

HCC, hepatocellular carcinoma.

corresponding to biological regulation was the highest, accounting for approximately 60.6%. Genes related to cellular components and metabolic processes were expressed at approximately 18.0% and 17.9%, respectively. Additionally, genes related to the immune response and rhythmic processes were identified with expression levels of 6.9% (Fig. 2B). In the metabolic process group, the amine metabolic process showed the highest expression at approximately 39%, followed by the alcohol metabolic process, a key function of hepatocytes, at approximately 30%. In the biological regulation category, various expression patterns were observed, ranging from cell proliferation to response to stimulation. Notably, the highest expression difference was approximately 67% in the biological regulation part of the cell. Among the cellular components, which showed the third highest expression pattern, a high expression level of approximately 57% was observed in the structural-developmental part (Fig. 2C).

Enrichment protein network of HCC cells with CSC propensity

Analysis of the enrichment protein patterns among the biological regulation category, which showed high expression changes, revealed that the expression z-score of calcium ion binding-related proteins was higher than that of the CD133- type (Fig. 3A; Table 1). Among the 19 calcium ion binding proteins, 13 were observed in the functional annotation enrichment analysis. Correlation analysis of these 13 proteins confirmed that 10 of them have a close relationship with each other on the gene-to-gene network (https://string-db.org/) (Fig. 3B). Nearly all proteins forming these 13 networks are associated with tumor proliferation, metastasis, and suppression of the immune response and are closely linked with CSC survival, invasion, metastasis, and resistance to therapeutic drugs. In particular, the S100 family members MYL12B and TPT1, which are highly correlated with CD133+ status, were found to be closely associated with CSC infiltration and multidisciplinary resistance.

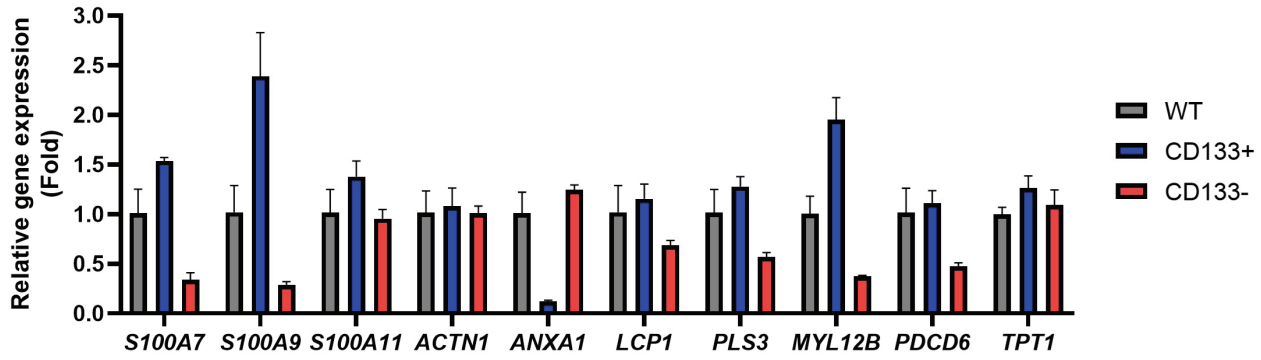

Figure 4. Comparison of the S100 family of CD133+ Huh7 over CD133- Huh7. Based on the protein network results with a high correlation to CD133+, we compared the actual expression levels and found that the S100 family members were more highly expressed in CD133+ cells than in the wild-type cells, whereas their expression was lower in CD133- cells than in wild-type cells. Conversely, ANXA1 was barely expressed in CD133+, while its expression increased in CD133- cells, compared to wild-type, although not significantly. WT, wild type.

Comparison of the S100 family of CD133+ Huh7 over CD133- Huh7

To confirm the effect of proteomic profiling on actual expression, the expression patterns of ten closely related calcium ion-binding proteins in the CD133+ and CD133- groups were compared relative to the wild-type cells (Fig. 4). Among the calcium-binding proteins, the S100 family was highly expressed in CD133+ cells, with MYL12B and TPT1 also showing significantly higher expression (P<0.05, P<0.01). Although not significant, LCP1, PLS3, and PDCD6 also exhibited higher expression levels compared to the wild-type cells, displaying an expression pattern opposite to that of CD133-. Conversely, ANXA1 expression was significantly suppressed in CD133+ cells compared to both wild-type and CD133- cells (P<0.01), while ACTN1 did not show a significant difference among the three groups.

DISCUSSION

CSCs represent a subpopulation of tumor cells capable of proliferation, self-renewal, and differentiation into more specialized tumor cells, which collectively form the tumor mass.[5,7] These cells are believed to be crucial for the sustained growth of malignant tumors and are implicated in cancer resistance to conventional therapies and tumor recurrence.[11,12] Among the various dysregulated mechanisms in tumors, those involving Ca^{2+} play a significant role in several facets of cancer progression.[9,16] Ca^{2+} serves as a ubiquitous secondary messenger with its intracellular concentration tightly regulated by channels, pumps, exchangers, and Ca^{2+}-binding proteins.[16]

In 1965, Moore isolated a protein from the bovine brain and identified proteins specific to the nervous system.[17] This protein, named S-100, derived its name from its solubility in 100% saturated ammonium sulfate at neutral pH.[17] Subsequent work by Isobe et al.[18] revealed that S100 forms a dimer composed of two homologous yet distinct subunits, known as S100A and S100B.[19] Over the years, research has demonstrated that the expression of S100 protein extends beyond nervous tissue and is present in various vertebrate tissues.[16,20] To date, 25 members of the S100 family have been identified.[21]

Among these, S100A7, S100A9, and S100A11, identified in this study, are known to have different influences on cancer proliferation and development, with A9 in particular being strongly associated with the immune evasion of CSCs.[22]

The S100 family comprises a group of calcium-binding proteins overexpressed in HCC and other liver diseases.[21] Recent literature suggests that S100 proteins play a crucial role in the development and progression of HCC and other cancers, including CSCs.[22] Specifically, the critical role of the S100 protein family in CSC involves complex mechanisms such as cancer stemness remodeling, anaerobic glycolysis regulation, tumor-associated macrophage differentiation, and epithelial-mesenchymal transition (EMT).[22]

S100A7 (psoriasin) is a relatively recent addition to the S100 gene family, initially identified as an 11.4 kDa protein expressed in squamous epithelial cells of psoriatic skin.[23] The S100 gene family encodes small cytoplasmic and secreted proteins characterized by EF-hand helix-loop-helix domains that are essential for calcium-binding functions and are implicated in various cellular processes, including growth, differentiation, and cell shape determination.[24] Notably, recent research has linked S100A7 expression in invasive breast tumors to poor clinical outcomes, even among high-risk subgroups of estrogen receptor (ER)-negative tumors.[14] S100A9 (calgranulin B, MRP14) is a member of

the S100 family of Ca^{2+}-binding proteins.[16,22] It predominantly exists as part of a heterodimer because homodimers are rare owing to their limited stability.[25] S100A9 is constitutively expressed in neutrophils and monocytes, where it functions as a Ca^{2+} sensor and plays a key role in cytoskeletal rearrangement and arachidonic acid metabolism.[22] Recent studies have revealed that S100A9 is upregulated in several cancers, including invasive ductal carcinoma of the breast, colitis-associated colon cancer, and HCC, and its expression is correlated with poor patient prognosis.[26] Furthermore, tumor-associated macrophages (TAMs) can enhance the expression of S100A9, promoting stem cell-like traits in HCC cells.[22,25]

S100A11, a member of the S100 protein family, mediates signaling pathways triggered by internal or external stimuli and plays a role in various diseases, including cancer, metabolic disorders, neurological conditions, and vascular calcification.[21,27] Its expression is significantly elevated in tumors and is associated with cancer progression and poor outcomes, showing a positive correlation with tumor size and cancer advancement and a negative correlation with disease-free survival rates.[27,28] Studies have demonstrated that S100A11 upregulation enhances tumor cell proliferation, migration, and invasion by activating multiple signaling pathways.[28] For instance, the A-S100A11/ANXA2 complex facilitates plasma membrane resealing following damage caused by metastatic tissue invasion, while silencing S100A11 in intrahepatic cholangiocarcinoma inhibits transforming growth factor-β1 (TGF-β1)-induced cell migration, invasion, and EMT.[29,30]

Based on their expression profiles, S100 proteins are emerging as potentially useful diagnostic and prognostic biomarkers.

The myosin regulatory subunit, MYL12B, is crucial for controlling contractile activity in both smooth muscle and nonmuscle cells through phosphorylation.[10,31] This phosphorylation event facilitates actin polymerization in vascular smooth muscle[32] and plays a role in cytokinesis, receptor capping, and cell migration.[32] However, its association with cancer remains largely unexplored, highlighting the need for further investigation into its role in cancer cell metastasis.

tumor protein, translationally-controlled 1 (TPT1/TCTP) is highly expressed in tumor cells and is implicated in various cellular functions, including protein synthesis, cell growth, and survival.[33] This highly conserved multifunctional protein regulates numerous cellular activities, including proliferation, growth, and metabolism, and is frequently overexpressed in various tumor types.[34,35] Recent studies have identified TPT1 as a direct target of the tumor suppressor TP53/p53, linking it to cell survival regulation and the promotion of proliferation in brain tumor-initiating cells, a process influenced by macrophage migration inhibitory factor (MIF).[36]

In contrast, annexin 1 (ANXA1), which plays a role in the development and progression of triple-negative breast cancer (TNBC) and is associated with poor patient outcomes,[37] exhibits a strong correlation with calcium-binding proteins in the enriched protein network observed in the profiling results related to CSCs.[37,38] Despite this connection, the actual expression pattern revealed that the CD133+ type exhibited lower expression levels than the wild-type. Although ANXA1 has been identified in the literature, its effects on tumor stem cells, which have a major impact on tumor proliferation[39] and regulation of the tumor microenvironment,[40] require further investigation. Whether the decreased expression of ANXA1 is specific to CSCs or cancer cells with CSC propensity remains to be confirmed.

These findings indicate a strong correlation between CSCs, calcium-binding proteins, and cancer survival and metastasis. Notably, the S100 family is expected to serve as a promising diagnostic marker for CSCs.[4,9,12,16] Further research is required to explore the association between S100 family expression (via liquid biopsy) and clinical outcomes, such as survival and recurrence in circulating tumor cells, to establish its potential as a diagnostic marker.

Conflicts of Interest

The authors have no conflicts of interest to disclose.

Ethics Statement

Experiments with commercially available cell lines are not IRB-approved.

Funding Statement

This study was supported by a faculty research grant of Yonsei University College of Medicine for 2015 (6-2015-0028).

Data Availability

All data generated or analyzed during this study are included in this article. Further enquiries can be directed to the corresponding author.

ORCID

Sung Hoon Choi https://orcid.org/0000-0002-3304-649X
Ha Young Lee https://orcid.org/0000-0001-7778-4921
Sung Ho Yun https://orcid.org/0009-0002-6775-7182
Sung Jae Jang https://orcid.org/0000-0001-7654-7326
Seung Up Kim https://orcid.org/0000-0002-9658-8050

Jun Yong Park https://orcid.org/0000-0001-7048-9153
Sang Hoon Ahn https://orcid.org/0000-0002-7642-5342
Do Young Kim https://orcid.org/0000-0002-8327-3439

Author Contributions

Conceptualization: SHC, SHA, DYK
Data curation: SHC
Formal analysis: SHC, HYL, SHY, SJJ
Project administration: SHC, DYK
Supervision: DYK
Validation: SHY, SUK, JYP, SHA, DYK
Visualization: HYL, SJJ
Writing - original draft: SHC, SJJ
Writing - review & editing: SUK, JYP, SHA, DYK

Supplementary Material

Supplementary data can be found with this article online https://doi.org/10.17998/jlc.2025.03.08.

REFERENCES

1. Wang N, Wang S, Li MY, Hu BG, Liu LP, Yang SL, et al. Cancer stem cells in hepatocellular carcinoma: an overview and promising therapeutic strategies. Ther Adv Med Oncol 2018;10:1758835918816287.
2. Choi SH, Lee SW, Ok M, Kim KS, Kim S, Ahn SH. Gene expression profiling of hepatocellular carcinoma derived cancer stem like cell under hypoxia. Yonsei Med J 2017;58:925-933.
3. Liu YC, Yeh CT, Lin KH. Cancer stem cell functions in hepatocellular carcinoma and comprehensive therapeutic strategies. Cells 2020;9:1331.
4. Ma S. Biology and clinical implications of CD133(+) liver cancer stem cells. Exp Cell Res 2013;319:126-132.
5. Collins CA, Olsen I, Zammit PS, Heslop L, Petrie A, Partridge TA, et al. Stem cell function, self-renewal, and behavioral heterogeneity of cells from the adult muscle satellite cell niche. Cell 2005;122:289-301.
6. Carnero A, Garcia-Mayea Y, Mir C, Lorente J, Rubio IT, LLeonart ME. The cancer stem-cell signaling network and resistance to therapy. Cancer Treat Rev 2016;49:25-36.
7. Huang T, Song X, Xu D, Tiek D, Goenka A, Wu B, et al. Stem cell programs in cancer initiation, progression, and therapy resistance. Theranostics 2020;10:8721-8743.
8. Lord CJ, Ashworth A. The DNA damage response and cancer therapy. Nature 2012;481:287-294.
9. Yin W, Wang J, Jiang L, Kang YJ. Cancer and stem cells. Exp Biol Med (Maywood) 2021;246:1791-1801.
10. Dzobo K, Senthebane DA, Ganz C, Thomford NE, Wonkam A, Dandara C. Advances in therapeutic targeting of cancer stem cells within the tumor microenvironment: an updated review. Cells 2020;9:1896.
11. Lee TK, Guan XY, Ma S. Cancer stem cells in hepatocellular carcinoma - from origin to clinical implications. Nat Rev Gastroenterol Hepatol 2022;19:26-44.
12. Nio K, Yamashita T, Kaneko S. The evolving concept of liver cancer stem cells. Mol Cancer 2017;16:4.
13. Vieira CP, McCarrel TM, Grant MB. Novel methods to mobilize, isolate, and expand mesenchymal stem cells. Int J Mol Sci 2021;22:5728.
14. Emberley ED, Murphy LC, Watson PH. S100A7 and the progression of breast cancer. Breast Cancer Res 2004;6:153-159.
15. Ishihama Y, Oda Y, Tabata T, Sato T, Nagasu T, Rappsilber J, et al. Exponentially modified protein abundance index (emPAI) for estimation of absolute protein amount in proteomics by the number of sequenced peptides per protein. Mol Cell Proteomics 2005;4:1265-1272.
16. Terrié E, Coronas V, Constantin B. Role of the calcium toolkit in cancer stem cells. Cell Calcium 2019;80:141-151.
17. Shashoua VE, Hesse GW, Moore BW. Proteins of the brain extracellular fluid: evidence for release of S-100 protein. J Neurochem 1984;42:1536-1541.
18. Isobe T, Okuyama T. The amino-acid sequence of the alpha subunit in bovine brain S-100a protein. Eur J Biochem 1981;116:79-86.
19. Baudier J, Gerard D. Ions binding to S100 proteins. II. Conformational studies and calcium-induced conformational changes in S100 alpha alpha protein: the effect of acidic pH and calcium incubation on subunit exchange in S100a (alpha beta) protein. J Biol Chem 1986;261:8204-8212.
20. Watanabe T, Okumura T, Hirano K, Yamaguchi T, Sekine S, Nagata T, et al. Circulating tumor cells expressing cancer stem cell marker CD44 as a diagnostic biomarker in patients with gastric cancer. Oncol Lett 2017;13:281-288.
21. Zhang C, Yao R, Chen J, Zou Q, Zeng L. S100 family members: potential therapeutic target in patients with hepatocellular carcinoma: a STROBE study. Medicine (Baltimore) 2021;100:e24135.
22. Markowitz J, Carson WE 3rd. Review of S100A9 biology and its role in cancer. Biochim Biophys Acta 2013;1835:100-109.
23. Granata M, Skarmoutsou E, Mazzarino MC, D'Amico F. S100A7 in psoriasis: immunodetection and activation by CRISPR technology. Methods Mol Biol 2019;1929:729-738.
24. Tian T, Li X, Hua Z, Ma J, Wu X, Liu Z, et al. S100A7 promotes the migration, invasion and metastasis of human cervical cancer cells through epithelial-mesenchymal transition. Oncotarget 2017;8:24964-24977.
25. Wei R, Zhu WW, Yu GY, Wang X, Gao C, Zhou X, et al. S100 calcium-binding protein A9 from tumor-associated macrophage enhances cancer stem cell-like properties of hepatocellular carcinoma. Int J Cancer 2021;148:1233-1244.
26. Duan L, Wu R, Ye L, Wang H, Yang X, Zhang Y, et al. S100A8 and S100A9 are associated with colorectal carcinoma progression and contribute to colorectal carcinoma cell survival and migration via Wnt/β-catenin pathway. PLoS One 2013;8:e62092.
27. Zhang L, Zhu T, Miao H, Liang B. The calcium binding protein S100A11 and its roles in diseases. Front Cell Dev Biol 2021;9:693262.
28. Cui Y, Li L, Li Z, Yin J, Lane J, Ji J, et al. Dual effects of targeting S100A11 on suppressing cellular metastatic properties and sensitizing drug response in gastric cancer. Cancer Cell Int 2021;21:243.
29. Tu Y, Xie P, Du X, Fan L, Bao Z, Sun G, et al. S100A11 functions as novel oncogene in glioblastoma via S100A11/ANXA2/NF-κB positive feedback loop. J Cell Mol Med 2019;23:6907-6918.
30. Zhang MX, Gan W, Jing CY, Zheng SS, Yi Y, Zhang J, et al. S100A11 promotes cell proliferation via P38/MAPK signaling pathway in intrahepatic cholangiocarcinoma. Mol Carcinog 2019;58:19-30.
31. Wu F, Dong XJ, Li YY, Zhao Y, Xu QL, Su L. Identification of phosphorylated MYL12B as a potential plasma biomarker for septic acute kidney injury using a quantitative proteomic approach. Int J Clin Exp Pathol 2015;8:14409-14416.
32. Chen X, Pavlish K, Benoit JN. Myosin phosphorylation triggers actin polymerization in vascular smooth muscle. Am J Physiol Heart Circ Physiol 2008;295:H2172-H2177.
33. Morimoto Y, Tokumitsu A, Sone T, Hirota Y, Tamura R, Sakamoto A, et al. TPT1 supports proliferation of neural stem/progenitor cells and brain tumor initiating cells regulated by macrophage migration inhibitory factor (MIF). Neurochem Res 2022;47:2741-2756.
34. Bae SY, Byun S, Bae SH, Min DS, Woo HA, Lee K. TPT1 (tumor protein, translationally-controlled 1) negatively regulates autophagy through the BECN1 interactome and an MTORC1-mediated pathway. Autophagy 2017;13:820-833.

35. Neuhäuser K, Küper L, Christiansen H, Bogdanova N. Assessment of the role of translationally controlled tumor protein 1 (TPT1/TCTP) in breast cancer susceptibility and ATM signaling. Clin Transl Radiat Oncol 2019;15:99-107.
36. Chen W, Wang H, Tao S, Zheng Y, Wu W, Lian F, et al. Tumor protein translationally controlled 1 is a p53 target gene that promotes cell survival. Cell Cycle 2013;12:2321-2328.
37. Okano M, Oshi M, Butash AL, Katsuta E, Tachibana K, Saito K, et al. Triple-negative breast cancer with high levels of annexin A1 expression is associated with mast cell infiltration, inflammation, and angiogenesis. Int J Mol Sci 2019;20:4197.
38. Johnstone CN, Tu Y, Langenbach S, Baloyan D, Pattison AD, Lock P, et al. Annexin A1 Is required for efficient tumor initiation and cancer stem cell maintenance in a model of human breast cancer. Cancers (Basel) 2021;13:1154.
39. Al-Ali HN, Crichton SJ, Fabian C, Pepper C, Butcher DR, Dempsey FC, et al. A therapeutic antibody targeting annexin-A1 inhibits cancer cell growth in vitro and in vivo. Oncogene 2024;43:608-614.
40. Li L, Wang B, Zhao S, Xiong Q, Cheng A. The role of ANXA1 in the tumor microenvironment. Int Immunopharmacol 2024;131:111854.